

Computation Set 06 Solution

AAE 440: Spacecraft Attitude Dynamics

Spring 2022

Due Date: May 02, 2022

Brendan Gillis

Problem 01: Problem Statement

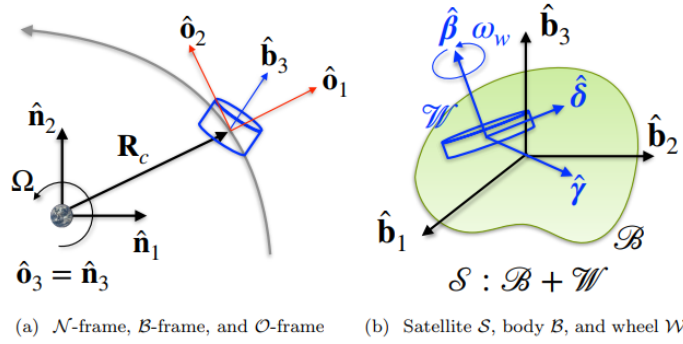


Figure 1: Dual-spin satellite in a circular orbit

In this problem, we investigate the attitude motion of dual-spin satellites analytically and numerically. Consider a satellite in a circular orbit about Earth ($\mu = 3.9860 \times 10^5 \text{ km}^3/\text{s}^2$) of orbit radius $R = 6500 \text{ [km]}$.

Fig. 1(a) describes the usual frames considered in this problem. The inertial frame, satellite body-fixed frame, and orbit frame are represented by \mathcal{N} -frame, \mathcal{B} -frame, and \mathcal{O} -frame, where $\{\hat{n}_1, \hat{n}_2, \hat{n}_3\}$, $\{\hat{b}_1, \hat{b}_2, \hat{b}_3\}$, and $\{\hat{o}_1, \hat{o}_2, \hat{o}_3\}$ are right-handed vector bases fixed in \mathcal{N} -frame, \mathcal{B} -frame, and \mathcal{O} -frame, respectively. \mathcal{N} -frame and \mathcal{O} -frame are taken so that the orbit lies in the plane spanned by \hat{n}_1 and \hat{n}_2 , $\hat{n}_3 = \hat{o}_3$, and that the orbit radius vector \mathbf{R}_c is aligned with \hat{o}_1 , i.e., $\mathbf{R}_c = R_c \hat{o}_1$. Denote the orbit angular speed by Ω .

As illustrated in Fig. 1(b), the dual-spin satellite \mathcal{S} is equipped with an axisymmetric wheel \mathcal{W} , whose spin axis is fixed in the satellite body \mathcal{B} . The inertia properties of the satellite and wheel are expressed via $\bar{\mathbf{I}}_s$ and $\bar{\mathbf{I}}_w$ as:

$$\bar{\mathbf{I}}_s = I_1 \hat{b}_1 \hat{b}_1 + I_2 \hat{b}_2 \hat{b}_2 + I_3 \hat{b}_3 \hat{b}_3, \quad \bar{\mathbf{I}}_w = K \hat{\gamma} \hat{\gamma} + K \hat{\delta} \hat{\delta} + J \hat{\beta} \hat{\beta} \quad (1)$$

The angular velocity of \mathcal{B} -frame relative to \mathcal{N} -frame and \mathcal{W} -frame relative to \mathcal{B} -frame are expressed as:

$$\boldsymbol{\omega}_{B/N} = \omega_1 \hat{b}_1 + \omega_2 \hat{b}_2 + \omega_3 \hat{b}_3, \quad \boldsymbol{\omega}_{W/B} = \omega_w \hat{\beta}, \quad \hat{\beta} = \beta_1 \hat{b}_1 + \beta_2 \hat{b}_2 + \beta_3 \hat{b}_3 \quad (2)$$

where the wheel spin axis $\hat{\beta}$ is constant in \mathcal{B} -frame (i.e., $\dot{\beta}_i = 0$) because the wheel is fixed in the body. In addition, assume that the wheel is rotating at a constant speed, and that the spin axis is aligned with \hat{b}_3 .

- For a set of kinematic variables of your choice (other than Euler parameters, which were already discussed in class), **derive** a set of nonlinear differential equations (both kinematic and dynamic equations) that describe the satellite's attitude motion under the action of gravity gradient torque.
- Show** that an orbit relative equilibrium state, given by $\hat{b}_i = \hat{o}_i$, is a particular solution of the differential equations derived in the previous question.
- Perform** the linearization of the differential equations about the particular solution and **derive** the characteristic equations.
- Let us assess the stability of the attitude motion for various satellite inertia properties. For each of the satellites with the following inertia properties, **show** the two types of stability charts discussed in class (i.e., values of b , c , and $b^2 - 4c$ as functions of ω_w/Ω and values of λ_i as functions of ω_w/Ω), where take the range of the horizontal axis to be $[-3I_1/J, 3I_1/J]$.
 - $\{I_1, I_2, I_3, J\} = \{700, 800, 500, 0.05\} \text{ kg} \cdot \text{m}^2$
 - $\{I_1, I_2, I_3, J\} = \{540, 800, 500, 0.05\} \text{ kg} \cdot \text{m}^2$
 - $\{I_1, I_2, I_3, J\} = \{500, 800, 700, 0.05\} \text{ kg} \cdot \text{m}^2$
 - $\{I_1, I_2, I_3, J\} = \{500, 700, 800, 0.05\} \text{ kg} \cdot \text{m}^2$
 - $\{I_1, I_2, I_3, J\} = \{800, 500, 700, 0.05\} \text{ kg} \cdot \text{m}^2$
- Discuss** the results of the linear stability for each inertia case, addressing the following points:
 - which region of Fig. 2 corresponds to each inertia case when the wheel is not spinning, and its implication in terms of stability
 - how the stability of the dual-spin satellite changes as ω_w varies; what values of ω_w/Ω yield unstable motions: why?

(f): **Optional** (extra credit for *both* AAE 440 and 590)

Discuss how the unstable region would change if we consider a different value of J while keeping the values of I_i same. (Hint: The functional structures of b and c in the characteristic equations imply that similar plots can be drawn by using $J\omega_w/\Omega$ instead of ω_w/Ω)

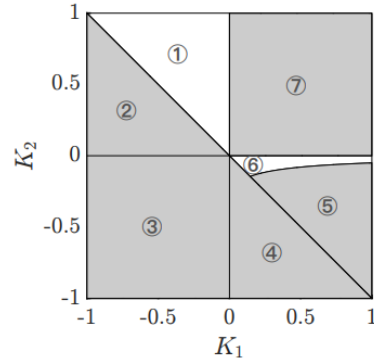


Figure 2: Stability chart for satellites with no spinning wheels

Numerical Investigation: Let us now numerically investigate the nonlinear attitude motion and compare the results against the linear stability analysis. Note that the orbit radius considered is

different from previous problem sets, $R = 6500$ [km]. The initial conditions with small errors are given in terms of the principal rotation as follows:

$$\hat{\lambda}(t=0) = \frac{1}{\sqrt{3}}(\hat{b}_1 + \hat{b}_2 + \hat{b}_3), \quad \theta(t=0) = \theta_0, \quad (3)$$

which needs to be converted to the kinematic variables of your choice.

(g): Answer the following questions for *each case* considered in part (d).

(g.1): Based on the result of linear stability analysis, pick a value of ω_w that yields linear marginal stability, and **report** the value in rpm (revolutions per minute). If there is no such ω_w that stabilizes the system, choose a spin speed that gives the minimum number of unstable eigenvalues. **Discuss** if the chosen ω_w is practically feasible (Note: maximum rotation speed of typical reaction wheels is around several thousands rpm).

(g.2): Suppose that the initial attitude error in Eq. (3) is given by $\theta_0 = 3$ deg = $\pi/60$ rad. Numerically integrate the differential equations derived in part (a) for a time span from $t = 0$ to $t = 24$ [hours] with integration tolerance 1.0×10^{-10} , and **show** the plots of the dependent variables over time.

(g.3): **Compute** the principal rotation angle $\theta(t)$, and **show** $\theta(t)$ in degrees as a function of time.

(g.4): **Discuss** the obtained numerical results, addressing the following points:

- how do the dependent variables and $\theta(t)$ behave over time?
- the maximum value of θ over time; how does it compare against the initial error θ_0 ?
- does the numerical result agree with the result of the linear stability analysis (to the extent we can tell from the conducted numerical simulations)?

(h): **Repeat** the same investigation (g.2)-(g.4) for different ω_w which, this time, you choose to yield unstable motion, for *each case* considered in part (d). If there is no such ω_w that stabilizes the system, choose a spin speed that yields a different number of unstable eigenvalues. **Discuss** the result following the guides in part (g.4).

Problem 01: Problem Solution

Part (a):

For this derivation we will use Modified Rodrigues Parameters to determine our equations of motion.

Kinematics:

$$\begin{bmatrix} \dot{\sigma}_1 \\ \dot{\sigma}_2 \\ \dot{\sigma}_3 \end{bmatrix} = \frac{1}{4} \begin{bmatrix} 1 - \sigma^2 + 2\sigma_1^2 & 2(\sigma_1\sigma_2 - \sigma_3) & 2(\sigma_1\sigma_2 + \sigma_2) \\ 2(\sigma_2\sigma_1 + \sigma_3) & 1 - \sigma^2 + 2\sigma_2^2 & 2(\sigma_2\sigma_3 - \sigma_1) \\ 2(\sigma_3\sigma_1 - \sigma_2) & 2(\sigma_3\sigma_2 + \sigma_1) & 1 - \sigma^2 + 2\sigma_3^2 \end{bmatrix} \begin{bmatrix} \omega_1 \\ \omega_2 \\ (\omega_3 + \Omega) \end{bmatrix}$$

$$\begin{cases} 4\dot{\sigma}_1 = (1 - \sigma^2 + 2\sigma_1^2)\omega_1 + 2(\sigma_1\sigma_2 - \sigma_3)\omega_2 + 2(\sigma_1\sigma_2 + \sigma_2)(\omega_3 + \Omega) \\ 4\dot{\sigma}_2 = 2(\sigma_2\sigma_1 + \sigma_3)\omega_1 + (1 - \sigma^2 + 2\sigma_2^2)\omega_2 + 2(\sigma_2\sigma_3 - \sigma_1)(\omega_3 + \Omega) \\ 4\dot{\sigma}_3 = 2(\sigma_3\sigma_1 - \sigma_2)\omega_1 + 2(\sigma_3\sigma_2 + \sigma_1)\omega_2 + (1 - \sigma^2 + 2\sigma_3^2)(\omega_3 + \Omega) \end{cases}$$

Next we can derive the dynamical equations noting that only the gravity gradient term is attitude dependent. There we can write our \mathbf{R} vector using the DCM as a function of our MRP. Finally, we assume the wheel rotates at constant speed and about $\hat{\mathbf{b}}_3$

Dynamics:

$$\begin{bmatrix} \dot{\omega}_1 \\ \dot{\omega}_2 \\ \dot{\omega}_3 \end{bmatrix} = \begin{bmatrix} K_1\omega_2\omega_3 \\ K_2\omega_1\omega_3 \\ K_3\omega_1\omega_2 \end{bmatrix} - \begin{bmatrix} \frac{J}{I_1} [\dot{\omega}_w\beta_1 - \omega_w(\beta_2\omega_3 - \beta_3\omega_2)] \\ \frac{J}{I_2} [\dot{\omega}_w\beta_2 - \omega_w(\beta_3\omega_1 - \beta_1\omega_3)] \\ \frac{J}{I_3} [\dot{\omega}_w\beta_3 - \omega_w(\beta_1\omega_2 - \beta_2\omega_1)] \end{bmatrix} - \frac{3\Omega^2}{\|\mathbf{R}_c\|_2^2} \begin{bmatrix} K_1R_3R_2 \\ K_2R_1R_3 \\ K_3R_2R_1 \end{bmatrix}$$

$$\beta_1 = \beta_2 = 0, \quad \beta_3 = 1, \quad \dot{\omega}_w = 0$$

$$\begin{bmatrix} \dot{\omega}_1 \\ \dot{\omega}_2 \\ \dot{\omega}_3 \end{bmatrix} = \begin{bmatrix} K_1\omega_2\omega_3 \\ K_2\omega_1\omega_3 \\ K_3\omega_1\omega_2 \end{bmatrix} + \begin{bmatrix} -\frac{J}{I_1} \omega_w\omega_2 \\ \frac{J}{I_2} \omega_w\omega_1 \\ 0 \end{bmatrix} - \frac{3\Omega^2}{\|\mathbf{R}_c\|_2^2} \begin{bmatrix} K_1R_3R_2 \\ K_2R_1R_3 \\ K_3R_2R_1 \end{bmatrix}$$

$$\begin{bmatrix} R_1 \\ R_2 \\ R_3 \end{bmatrix} = [\mathcal{B}\mathcal{O}]^o \mathbf{R} = \frac{1}{(1 + \sigma^2)^2} \begin{bmatrix} 4(\sigma_1^2 - \sigma_2^2 - \sigma_3^2) + (1 - \sigma^2)^2 & \sim & \sim \\ 8\sigma_2\sigma_1 - 4\sigma_3(1 - \sigma^2) & \sim & \sim \\ 8\sigma_3\sigma_1 + 4\sigma_2(1 - \sigma^2) & \sim & \sim \end{bmatrix} \begin{bmatrix} -R \\ 0 \\ 0 \end{bmatrix}$$

$$\frac{3\Omega^2}{\|\mathbf{R}_c\|_2^2} \begin{bmatrix} K_1R_3R_2 \\ K_2R_1R_3 \\ K_3R_2R_1 \end{bmatrix} = \frac{12\Omega^2}{(1 + \sigma^2)^4} \begin{bmatrix} K_1(8\sigma_2\sigma_1 - 4\sigma_3(1 - \sigma^2))(2\sigma_3\sigma_1 + \sigma_2(1 - \sigma^2)) \\ K_2(4(\sigma_1^2 - \sigma_2^2 - \sigma_3^2) + (1 - \sigma^2)^2)(2\sigma_3\sigma_1 + \sigma_2(1 - \sigma^2)) \\ K_3(2\sigma_2\sigma_1 - \sigma_3(1 - \sigma^2))(4(\sigma_1^2 - \sigma_2^2 - \sigma_3^2) + (1 - \sigma^2)^2) \end{bmatrix}$$

$$\begin{bmatrix} \dot{\omega}_1 \\ \dot{\omega}_2 \\ \dot{\omega}_3 \end{bmatrix} = \begin{bmatrix} K_1\omega_2\omega_3 \\ K_2\omega_1\omega_3 \\ K_3\omega_1\omega_2 \end{bmatrix} + \begin{bmatrix} -\frac{J}{I_1} \omega_w\omega_2 \\ \frac{J}{I_2} \omega_w\omega_1 \\ 0 \end{bmatrix} - \frac{3\Omega^2}{\|\mathbf{R}_c\|_2^2} \begin{bmatrix} K_1R_3R_2 \\ K_2R_1R_3 \\ K_3R_2R_1 \end{bmatrix},$$

$$\frac{3\Omega^2}{\|\mathbf{R}_c\|_2^2} \begin{bmatrix} K_1R_3R_2 \\ K_2R_1R_3 \\ K_3R_2R_1 \end{bmatrix} = \frac{12\Omega^2}{(1 + \sigma^2)^4} \begin{bmatrix} K_1(8\sigma_2\sigma_1 - 4\sigma_3(1 - \sigma^2))(2\sigma_3\sigma_1 + \sigma_2(1 - \sigma^2)) \\ K_2(4(\sigma_1^2 - \sigma_2^2 - \sigma_3^2) + (1 - \sigma^2)^2)(2\sigma_3\sigma_1 + \sigma_2(1 - \sigma^2)) \\ K_3(2\sigma_2\sigma_1 - \sigma_3(1 - \sigma^2))(4(\sigma_1^2 - \sigma_2^2 - \sigma_3^2) + (1 - \sigma^2)^2) \end{bmatrix}$$

Part (b):

Here we can show that the an orbit relative equilibrium state given by $\hat{\mathbf{b}}_i = \hat{\mathbf{o}}_i$ is a particular solution by direct substitution into the equations derived in Part (a).

$$\begin{aligned}
 [\mathcal{BO}] &= I_{3 \times 3} \rightarrow \bar{\sigma}_{\mathcal{B}/\mathcal{O}} = 0, \quad \bar{\omega}_{\mathcal{B}/\mathcal{O}} = 0 = \bar{\omega}' \\
 \begin{bmatrix} \dot{\sigma}_1 \\ \dot{\sigma}_2 \\ \dot{\sigma}_3 \end{bmatrix} &= \frac{1}{4} \begin{bmatrix} 1 - \sigma^2 + 2\sigma_1^2 & 2(\sigma_1\sigma_2 - \sigma_3) & 2(\sigma_1\sigma_2 + \sigma_2) \\ 2(\sigma_2\sigma_1 + \sigma_3) & 1 - \sigma^2 + 2\sigma_2^2 & 2(\sigma_2\sigma_3 - \sigma_1) \\ 2(\sigma_3\sigma_1 - \sigma_2) & 2(\sigma_3\sigma_2 + \sigma_1) & 1 - \sigma^2 + 2\sigma_3^2 \end{bmatrix} \begin{bmatrix} \omega'_1 \\ \omega'_2 \\ \omega'_3 \end{bmatrix} \\
 \begin{bmatrix} \dot{\bar{\sigma}}_1 \\ \dot{\bar{\sigma}}_2 \\ \dot{\bar{\sigma}}_3 \end{bmatrix}_{\mathcal{B}/\mathcal{O}} &= \frac{1}{4} \begin{bmatrix} 1 - \bar{\sigma}^2 + 2\bar{\sigma}_1^2 & 2(\bar{\sigma}_1\bar{\sigma}_2 - \bar{\sigma}_3) & 2(\bar{\sigma}_1\bar{\sigma}_2 + \bar{\sigma}_2) \\ 2(\bar{\sigma}_2\bar{\sigma}_1 + \bar{\sigma}_3) & 1 - \bar{\sigma}^2 + 2\bar{\sigma}_2^2 & 2(\bar{\sigma}_2\bar{\sigma}_3 - \bar{\sigma}_1) \\ 2(\bar{\sigma}_3\bar{\sigma}_1 - \bar{\sigma}_2) & 2(\bar{\sigma}_3\bar{\sigma}_2 + \bar{\sigma}_1) & 1 - \bar{\sigma}^2 + 2\bar{\sigma}_3^2 \end{bmatrix} \begin{bmatrix} 0 \\ 0 \\ 0 \end{bmatrix} \\
 \begin{bmatrix} \dot{\bar{\sigma}}_1 \\ \dot{\bar{\sigma}}_2 \\ \dot{\bar{\sigma}}_3 \end{bmatrix}_{\mathcal{B}/\mathcal{O}} &= \begin{bmatrix} 0 \\ 0 \\ 0 \end{bmatrix} \\
 \begin{bmatrix} \dot{\omega}_1 \\ \dot{\omega}_2 \\ \dot{\omega}_3 \end{bmatrix} &= \begin{bmatrix} K_1\omega_2\omega_3 \\ K_2\omega_1\omega_3 \\ K_3\omega_1\omega_2 \end{bmatrix} + \begin{bmatrix} -\frac{J}{I_1}\omega_w\omega_2 \\ \frac{J}{I_2}\omega_w\omega_1 \\ 0 \end{bmatrix} - \frac{12\Omega^2}{(1 + \sigma^2)^4} \begin{bmatrix} K_1(8\sigma_2\sigma_1 - 4\sigma_3(1 - \sigma^2))(2\sigma_3\sigma_1 + \sigma_2(1 - \sigma^2)) \\ K_2(4(\sigma_1^2 - \sigma_2^2 - \sigma_3^2) + (1 - \sigma^2)^2)(2\sigma_3\sigma_1 + \sigma_2(1 - \sigma^2)) \\ K_3(2\sigma_2\sigma_1 - \sigma_3(1 - \sigma^2))(4(\sigma_1^2 - \sigma_2^2 - \sigma_3^2) + (1 - \sigma^2)^2) \end{bmatrix} \\
 \begin{bmatrix} \dot{\bar{\omega}}_1 \\ \dot{\bar{\omega}}_2 \\ \dot{\bar{\omega}}_3 \end{bmatrix} &= \begin{bmatrix} K_1 0 \\ K_2 0 \\ K_3 0 \end{bmatrix} + \begin{bmatrix} -\frac{J}{I_1} 0 \\ \frac{J}{I_2} 0 \\ 0 \end{bmatrix} - \frac{12\Omega^2}{(1 + \sigma^2)^4} \begin{bmatrix} 0 \\ 0 \\ 0 \end{bmatrix} = \begin{bmatrix} 0 \\ 0 \\ 0 \end{bmatrix} \\
 \sigma &= 0, \quad \sigma = 0, \quad \dot{\sigma} = 0, \quad \bar{\omega} = \Omega \hat{\mathbf{b}}_3, \quad \bar{\omega}_{\mathcal{B}/\mathcal{O}} = 0
 \end{aligned}$$

Part (c):

To determine our linearized equations, we can write our σ and ω in terms of the particular solution and perturbation, then substitute into our equations from Part (b) and neglect 2^{nd} or higher order terms.

$$\sigma = \bar{\sigma} + \tilde{\sigma} = \tilde{\sigma}, \quad \omega = \bar{\omega} + \tilde{\omega} = \begin{bmatrix} \tilde{\omega}_1 \\ \tilde{\omega}_2 \\ \Omega + \tilde{\omega}_3 \end{bmatrix}$$

Kinematics:

$$\begin{aligned}
 \begin{bmatrix} \dot{\tilde{\sigma}}_1 \\ \dot{\tilde{\sigma}}_2 \\ \dot{\tilde{\sigma}}_3 \end{bmatrix} &= \frac{1}{4} \begin{bmatrix} 1 - \tilde{\sigma}^2 + 2\tilde{\sigma}_1^2 & 2(\tilde{\sigma}_1\tilde{\sigma}_2 - \tilde{\sigma}_3) & 2(\tilde{\sigma}_1\tilde{\sigma}_2 + \tilde{\sigma}_2) \\ 2(\tilde{\sigma}_2\tilde{\sigma}_1 + \tilde{\sigma}_3) & 1 - \tilde{\sigma}^2 + 2\tilde{\sigma}_2^2 & 2(\tilde{\sigma}_2\tilde{\sigma}_3 - \tilde{\sigma}_1) \\ 2(\tilde{\sigma}_3\tilde{\sigma}_1 - \tilde{\sigma}_2) & 2(\tilde{\sigma}_3\tilde{\sigma}_2 + \tilde{\sigma}_1) & 1 - \tilde{\sigma}^2 + 2\tilde{\sigma}_3^2 \end{bmatrix} \begin{bmatrix} \tilde{\omega}_1 \\ \tilde{\omega}_2 \\ \Omega + \tilde{\omega}_3 \end{bmatrix} = \frac{1}{4} \begin{bmatrix} 1 & -\tilde{\sigma}_3 & \tilde{\sigma}_2 \\ \tilde{\sigma}_3 & 1 & -\tilde{\sigma}_1 \\ -\tilde{\sigma}_2 & \tilde{\sigma}_1 & 1 \end{bmatrix} \begin{bmatrix} \tilde{\omega}_1 \\ \tilde{\omega}_2 \\ \Omega + \tilde{\omega}_3 \end{bmatrix} = \frac{1}{4} \begin{bmatrix} \tilde{\omega}'_1 \\ \tilde{\omega}'_2 \\ \tilde{\omega}'_3 \end{bmatrix} + \Omega \begin{bmatrix} \tilde{\sigma}_2 \\ -\tilde{\sigma}_1 \\ 0 \end{bmatrix} \\
 \begin{bmatrix} \dot{\tilde{\sigma}}_1 \\ \dot{\tilde{\sigma}}_2 \\ \dot{\tilde{\sigma}}_3 \end{bmatrix} &= \frac{1}{4} \begin{bmatrix} \tilde{\omega}'_1 \\ \tilde{\omega}'_2 \\ \tilde{\omega}'_3 \end{bmatrix} + \Omega \begin{bmatrix} \tilde{\sigma}_2 \\ -\tilde{\sigma}_1 \\ 0 \end{bmatrix}
 \end{aligned}$$

Dynamics:

$$\begin{bmatrix} \dot{\omega}_1 \\ \dot{\omega}_2 \\ \dot{\omega}_3 \end{bmatrix} = \begin{bmatrix} K_1 \omega_2 \omega_3 \\ K_2 \omega_1 \omega_3 \\ K_3 \omega_1 \omega_2 \end{bmatrix} + \begin{bmatrix} -\frac{J}{I_1} \omega_w \omega_2 \\ \frac{J}{I_2} \omega_w \omega_1 \\ 0 \end{bmatrix} - \frac{3\Omega^2}{\|\mathbf{R}_c\|_2^2} \begin{bmatrix} K_1 R_3 R_2 \\ K_2 R_1 R_3 \\ K_3 R_2 R_1 \end{bmatrix}$$

$$\begin{bmatrix} K_1 \omega_2 \omega_3 \\ K_2 \omega_1 \omega_3 \\ K_3 \omega_1 \omega_2 \end{bmatrix} = \begin{bmatrix} K_1 \tilde{\omega}_2 \tilde{\omega}_3 \\ K_2 \tilde{\omega}_1 \tilde{\omega}_3 \\ K_3 \tilde{\omega}_1 \tilde{\omega}_2 \end{bmatrix} = \begin{bmatrix} 0 \\ 0 \\ 0 \end{bmatrix}$$

$$\begin{bmatrix} -\frac{J}{I_1} \omega_w \omega_2 \\ \frac{J}{I_2} \omega_w \omega_1 \\ 0 \end{bmatrix} = \begin{bmatrix} -\frac{J}{I_1} \omega_w \tilde{\omega}_2 \\ \frac{J}{I_2} \omega_w \tilde{\omega}_1 \\ 0 \end{bmatrix}$$

Next, we determine our ${}^B\mathbf{R}$ after the perturbation by calculating the DCM using our perturbed state:

$$[BN] = \frac{1}{(1+\tilde{\sigma}^2)^2} \begin{bmatrix} 4(\tilde{\sigma}_1^2 - \tilde{\sigma}_2^2 - \tilde{\sigma}_3^2) + (1 - \tilde{\sigma}^2)^2 & 8\tilde{\sigma}_1\tilde{\sigma}_2 + 4\tilde{\sigma}_3(1 - \tilde{\sigma}^2) & 8\tilde{\sigma}_1\tilde{\sigma}_3 - 4\tilde{\sigma}_2(1 - \tilde{\sigma}^2) \\ 8\tilde{\sigma}_2\tilde{\sigma}_1 - 4\tilde{\sigma}_3(1 - \tilde{\sigma}^2) & 4(-\tilde{\sigma}_1^2 + \tilde{\sigma}_2^2 - \tilde{\sigma}_3^2) + (1 - \tilde{\sigma}^2)^2 & 8\tilde{\sigma}_2\tilde{\sigma}_3 + 4\tilde{\sigma}_1(1 - \tilde{\sigma}^2) \\ 8\tilde{\sigma}_3\tilde{\sigma}_1 + 4\tilde{\sigma}_2(1 - \tilde{\sigma}^2) & 8\tilde{\sigma}_3\tilde{\sigma}_2 - 4\tilde{\sigma}_1(1 - \tilde{\sigma}^2) & 4(-\tilde{\sigma}_1^2 - \tilde{\sigma}_2^2 + \tilde{\sigma}_3^2) + (1 - \tilde{\sigma}^2)^2 \end{bmatrix}$$

$${}^B\mathbf{R} = [BN]^N \mathbf{R} = \begin{bmatrix} 1 & 4\tilde{\sigma}_3 & -4\tilde{\sigma}_2 \\ -4\tilde{\sigma}_3 & 1 & 4\tilde{\sigma}_1 \\ 4\tilde{\sigma}_2 & -4\tilde{\sigma}_1 & 1 \end{bmatrix} \begin{bmatrix} -R_c \\ 0 \\ 0 \end{bmatrix} = \begin{bmatrix} -R_c \\ 4\tilde{\sigma}_3 R_c \\ -4\tilde{\sigma}_2 R_c \end{bmatrix}$$

$$\frac{3\Omega^2}{\|\mathbf{R}_c\|_2^2} \begin{bmatrix} K_1 R_3 R_2 \\ K_2 R_1 R_3 \\ K_3 R_2 R_1 \end{bmatrix} = \begin{bmatrix} 0 \\ 12K_2\Omega^2\tilde{\sigma}_2 \\ -12K_3\Omega^2\tilde{\sigma}_3 \end{bmatrix}$$

$$\begin{bmatrix} \dot{\tilde{\omega}}_1 \\ \dot{\tilde{\omega}}_2 \\ \dot{\tilde{\omega}}_3 \end{bmatrix} = \begin{bmatrix} \tilde{\omega}_2(K_1\Omega - J/I_1 \omega_w) \\ \tilde{\omega}_1(K_2\Omega + J/I_2 \omega_w) - 12K_2\Omega^2\tilde{\sigma}_2 \\ 12K_3\Omega^2\tilde{\sigma}_3 \end{bmatrix}, \quad \begin{bmatrix} \dot{\tilde{\sigma}}_1 \\ \dot{\tilde{\sigma}}_2 \\ \dot{\tilde{\sigma}}_3 \end{bmatrix} = \frac{1}{4} \begin{bmatrix} \tilde{\omega}_1 + \Omega\tilde{\sigma}_2 \\ \tilde{\omega}_2 - \Omega\tilde{\sigma}_1 \\ \tilde{\omega}_3 \end{bmatrix}$$

To find the characteristic equations for this system we can first identify that $\tilde{\sigma}_3$ and $\tilde{\omega}_3$ are decoupled from the rest of the system. We can separate and combine those. For the other 4 state variables we can write the system of ODEs in the form $\dot{\mathbf{x}} = \mathbf{A}\mathbf{x}$ and solve for its eigenvalues.

$$\dot{\tilde{\omega}}_3 = 12K_3\Omega^2\tilde{\sigma}_3, \quad \dot{\tilde{\sigma}}_3 = \frac{1}{4}\tilde{\omega}_3, \quad \ddot{\tilde{\sigma}}_3 = 3K_3\Omega^2\tilde{\sigma}_3, \quad \lambda^2 - 3K_3\Omega^2 = 0$$

$$\begin{bmatrix} \dot{\tilde{\sigma}}_1 \\ \dot{\tilde{\sigma}}_2 \\ \dot{\tilde{\omega}}_1 \\ \dot{\tilde{\omega}}_2 \end{bmatrix} = \begin{bmatrix} 0 & \Omega & 1/4 & 0 \\ -\Omega & 0 & 0 & 1/4 \\ 0 & 0 & 0 & (K_1\Omega - J/I_1 \omega_w) \\ 0 & -12K_2\Omega^2 & (K_2\Omega + J/I_2 \omega_w) & 0 \end{bmatrix} \begin{bmatrix} \tilde{\sigma}_1 \\ \tilde{\sigma}_2 \\ \tilde{\omega}_1 \\ \tilde{\omega}_2 \end{bmatrix}$$

$$\det(A - \lambda I_{4 \times 4}) = \lambda^4 + b\lambda^2 + c = 0$$

$$\begin{cases} \lambda^4 + b\lambda^2 + c = 0 \\ b = \Omega^2 \left[1 + 3K_2 - K_1K_2 - \frac{\omega_w}{\Omega} \left(\frac{J}{I_2} K_1 - \frac{J}{I_1} K_2 \right) + \left(\frac{\omega_w}{\Omega} \right)^2 \frac{J^2}{I_1 I_2} \right] \\ c = -\Omega^4 \left(K_1 - \frac{J}{I_1} \frac{\omega_w}{\Omega} \right) \left(4K_2 + \frac{J}{I_2} \frac{\omega_w}{\Omega} \right) \end{cases}$$

Part (d) and Part (e):

Here we can plot our 3 inequalities on one graph and notice that at any place where the lines drop below zero corresponds to a ω_w/Ω that violates the inequality resulting in an unstable system. Similarly, we can compute the eigen values corresponding to every ω_w/Ω noting that any ω_w/Ω value that results in a positive real part of the eigenvalue will also cause the system to be unstable.

```
# Part d
Is = [[7, 8, 5], [5.4, 8, 5], [5, 8, 7], [5, 7, 8], [8, 5, 7]]
for I in Is:
    I = [100*i for i in I]
    J = 0.05
    K1 = (I[1]-I[2])/I[0]
    K2 = (I[2]-I[0])/I[1]
    K3 = (I[0]-I[1])/I[2]

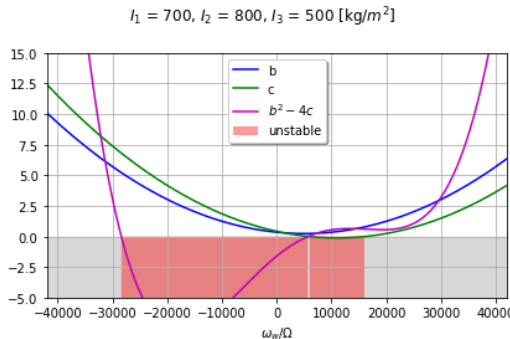
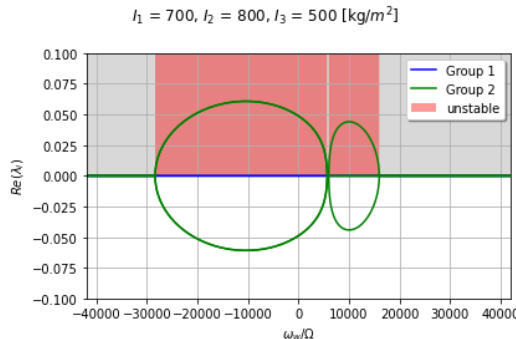
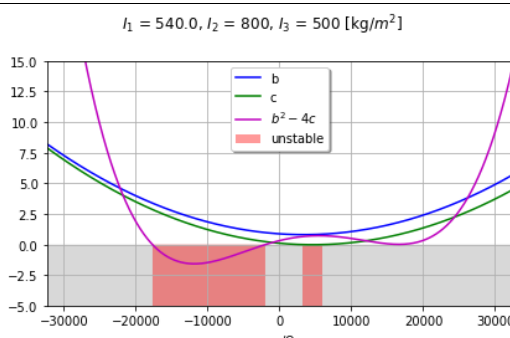
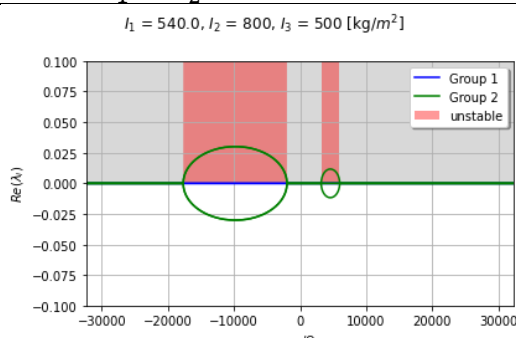
    Omega = 1
    u = np.linspace(-3*I[0]/J, 3*I[0]/J, 5000)

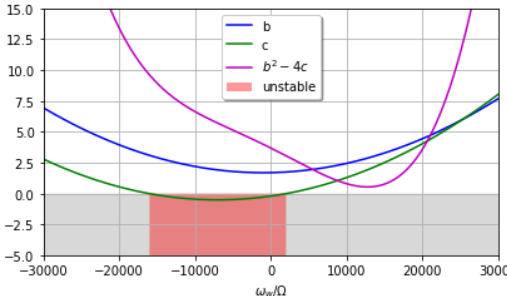
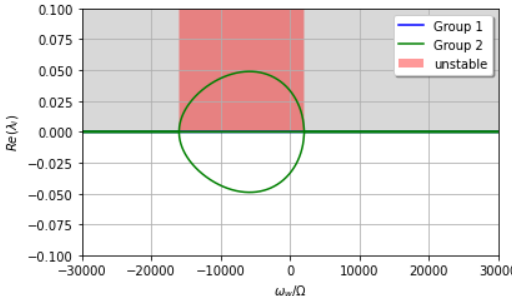
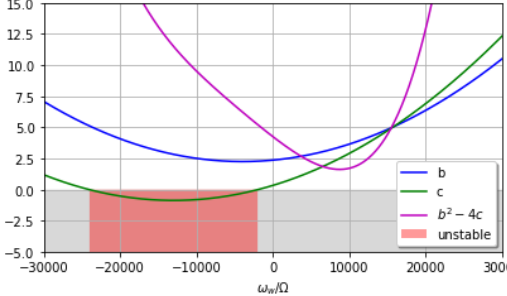
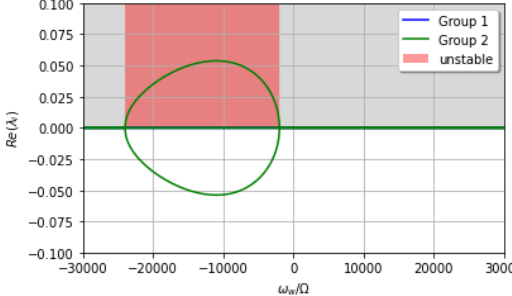
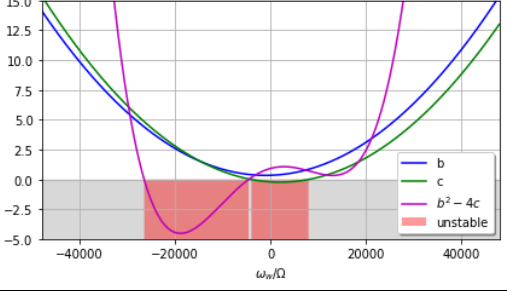
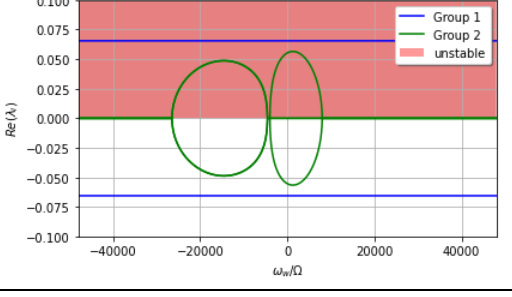
    b2 = J**2/(I[0]*I[1])*Omega**2
    b1 = (K2/I[0]-K1/I[1])*J*Omega**2
    b0 = (1+3*K2-K1*K2)*Omega**2

    c2 = J**2/(I[0]*I[1])*Omega**4
    c1 = (4*K2/I[0]-K1/I[1])*J*Omega**4
    c0 = -4*K1*K2*Omega**4

    b = b2*u**2+b1*u+b0
    c = c2*u**2+c1*u+c0

    roots1 = np.zeros([len(u), 2])
    roots2 = np.zeros([len(u), 4])
    for i, u1 in enumerate(u):
        roots1[i, :] = np.roots([1, 0, -K3*Omega**2])
        b = b2*u1**2+b1*u1+b0
        c = c2*u1**2+c1*u1+c0
        roots2[i, :] = np.roots([1, 0, b, 0, c])
```

d.1)	$I_1 = 700, I_2 = 800, I_3 = 500 \text{ [kg/m}^2\text{]}$ 	$I_1 = 700, I_2 = 800, I_3 = 500 \text{ [kg/m}^2\text{]}$ 
e.1) Region 5: Untable $\omega_w = 0, K_1 > 0, K_2 < 0, K_1 + K_2 > 0$	e.2) Unstable in for the $\frac{\omega_w}{\Omega}$ regions marked in red. Possible to stabilise system that do not violate $K_1 + K_2 < 0$	
d.2)	$I_1 = 540.0, I_2 = 800, I_3 = 500 \text{ [kg/m}^2\text{]}$ 	$I_1 = 540.0, I_2 = 800, I_3 = 500 \text{ [kg/m}^2\text{]}$ 
e.1) Region 6: Stable	e.2) Unstable in for the $\frac{\omega_w}{\Omega}$ regions marked in red. Possible to stabilise system that do not violate $K_1 + K_2 < 0$	

d.3)	<p>$I_1 = 500, I_2 = 800, I_3 = 700 \text{ [kg/m}^2\text{]}$</p> 	<p>$I_1 = 500, I_2 = 800, I_3 = 700 \text{ [kg/m}^2\text{]}$</p> 
	e.1) Region 7: Unstable	e.2) Unstable in for the $\frac{\omega_w}{\Omega}$ regions marked in red. Possible to stabilise system that do not violate $K_1 + K_2 < 0$
d.4)	<p>$I_1 = 500, I_2 = 700, I_3 = 800 \text{ [kg/m}^2\text{]}$</p> 	<p>$I_1 = 500, I_2 = 700, I_3 = 800 \text{ [kg/m}^2\text{]}$</p> 
	e.1) Region 1: Stable	e.2) Unstable in for the $\frac{\omega_w}{\Omega}$ regions marked in red. Possible to stabilise system that do not violate $K_1 + K_2 < 0$
d.5)	<p>$I_1 = 800, I_2 = 500, I_3 = 700 \text{ [kg/m}^2\text{]}$</p> 	<p>$I_1 = 800, I_2 = 500, I_3 = 700 \text{ [kg/m}^2\text{]}$</p> 
	e.1) Region 3: Unstable	e.2) Regions 1-3 are unstable from the K_i inequality so no change to wheel speed will change $K_1 + K_2 < 0$. Unstable for all $\frac{\omega_w}{\Omega}$

Part (g):

First let's calculate the our Ω for $R=6500\text{km}$:

$$v = \sqrt{\frac{\mu}{R}}, \quad \Omega = \frac{v}{2\pi R} = \frac{1}{2\pi} \sqrt{\frac{\mu}{R^3}} = 0.0115 \text{ rpm}$$

Part (g.1):

Part (g.1.1): 230 rpm: feasible ($\omega_w/\Omega = 20000$)

Part (g.1.2): 0 rpm: stable

Part (g.1.3): 56 rpm: feasible ($\omega_w/\Omega = 5000$)

Part (g.1.4): 0 rpm: stable

Part (g.1.5): 115 rpm: feasible but Unstable ($\omega_w/\Omega = 10000$)

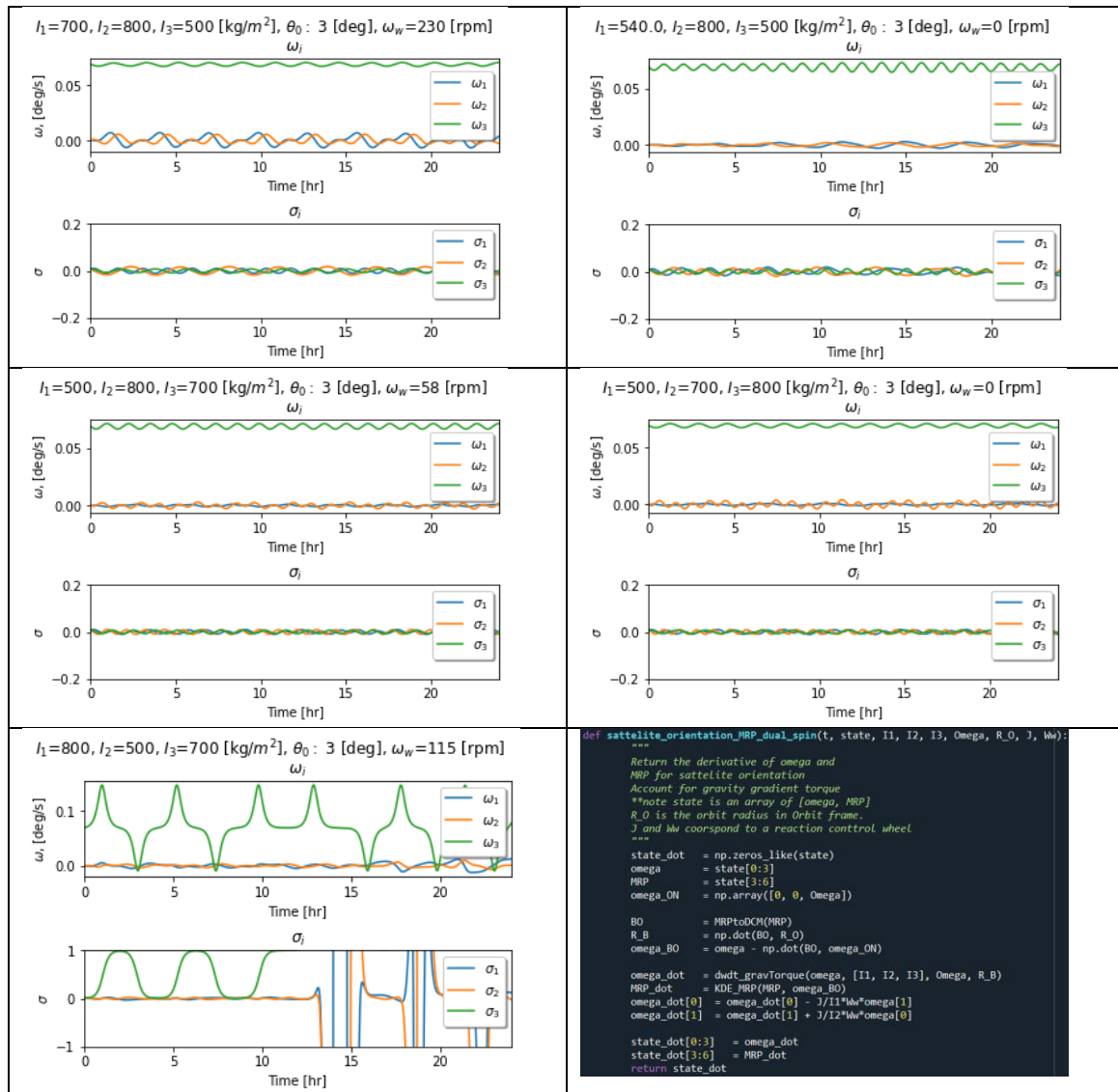
Part (g.2):

Several steps must be taken to numerically integrate the system. First, I calculate the radius vector in the B frame ${}^B\mathbf{R}$. Next, I calculate $\boldsymbol{\omega}'$. Finally, we can construct a state variable and integrate the orientation and angular velocity using the equations derived in Part (a).

$${}^B\mathbf{R} = [\mathcal{BO}(\boldsymbol{\sigma})]^O\mathbf{R} = [\mathcal{BO}(\boldsymbol{\sigma})] \begin{bmatrix} -R & 0 & 0 \end{bmatrix}^T$$

$${}^B\boldsymbol{\omega}' = {}^B\boldsymbol{\omega}_{B/O} - [\mathcal{BO}(\boldsymbol{\sigma})]^O\boldsymbol{\omega}_{O/N} = {}^B\boldsymbol{\omega}_{B/O} - [\mathcal{BO}(\boldsymbol{\sigma})] \begin{bmatrix} 0 & 0 & \Omega \end{bmatrix}^T$$

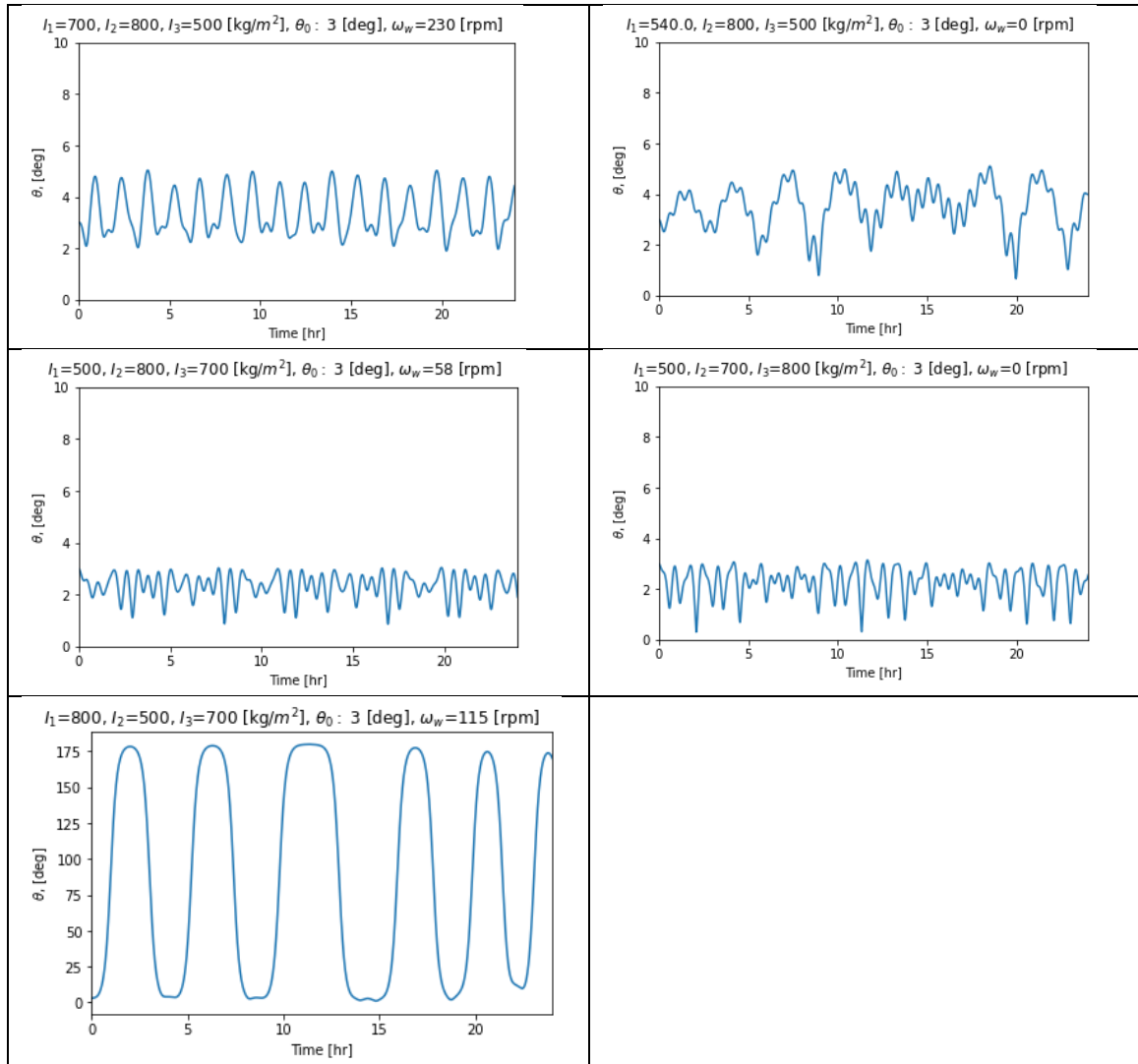
$$\begin{bmatrix} {}^B\dot{\boldsymbol{\omega}}_{B/O} \\ \dot{\boldsymbol{\sigma}} \end{bmatrix} = \begin{bmatrix} f(\boldsymbol{\omega}_{B/O}, \bar{\mathbf{I}}, {}^B\mathbf{R}) + g(\boldsymbol{\omega}_{B/O}, \bar{\mathbf{I}}, J, \omega_w) \\ h(\boldsymbol{\sigma}, \boldsymbol{\omega}_{B/O}) \end{bmatrix} = \begin{bmatrix} \text{dwdt_gravTorque() + spinTorque()} \\ \text{KDE_MRP()} \end{bmatrix}$$



Part (g.3):

Here in order to compute the angle associated with the principle axis of rotation I calculate the DCM, then the PRP from the DCM.

$$[\hat{\lambda}, \theta] = \text{DCMtoPRP}(\text{MRPtoDCM}(\sigma))$$

Part (g.4):Part (g.4.1):

- ω, σ, θ all remain very close to their initial values. Additionally both ω, σ appear periodic however do not follow a simple sinusoid.
- The maximum value of θ is 2 degrees higher than the initial perturbation.
- From the numerical simulation, we can say that this system agrees with our linear stability analysis which predicted that the system would be stable.

Part (g.4.2):

- ω, σ, θ all remain very close to their initial values. Additionally both ω, σ appear periodic however do not follow a simple sinusoid.
- The maximum value of θ is 2 degrees than the initial perturbation.
- From the numerical simulation, we can say that this system agrees with our linear stability analysis which predicted that the system would be stable.

Part (g.4.3):

- ω, σ, θ all remain very close to their initial values. Additionally both ω, σ appear periodic however do not follow a simple sinusoid.
- The maximum value of θ is 1% higher than the initial perturbation.
- From the numerical simulation, we can say that this system agrees with our linear stability analysis which predicted that the system would be stable.

Part (g.4.4):

- ω, σ, θ all remain very close to their initial values. Additionally both ω, σ appear periodic however do not follow a simple sinusoid.
- The maximum value of θ is 5% higher than the initial perturbation.
- From the numerical simulation, we can say that this system agrees with our linear stability analysis which predicted that the system would be stable.

Part (g.4.5):

- ω_3, σ_3 , and θ all vary significantly from their initial values and generally appear periodic. $\omega_{1,2}, \sigma_{1,2}$ remain very close to their initial values but do not show clear periodicity
- The maximum value of θ reaches 180 degrees – far higher than the perturbation
- From the numerical simulation, we can say that this system agrees with our linear stability analysis which predicted that the system would be unstable.
- It appears that as this body tumbled it neared the MRP singularity as evidenced by the massive jumps in σ_i to over 200 at points.

Part (h):

First let's calculate our Ω for $R=6500\text{km}$:

$$v = \sqrt{\frac{\mu}{R}}, \quad \Omega = \frac{v}{2\pi R} = \frac{1}{2\pi} \sqrt{\frac{\mu}{R^3}} = 0.0115 \text{rpm}$$

Part (h.1):

Part (h.1.1): 57 rpm: feasible ($\omega_w/\Omega = 5000$)

Part (h.1.2): -81rpm: feasible ($\omega_w/\Omega = -7000$)

Part (h.1.3): 35 rpm: feasible ($\omega_w/\Omega = -5000$)

Part (h.1.4): -57 rpm: stable

Part (h.1.5): -115 rpm: feasible but Unstable ($\omega_w/\Omega = -10000$)

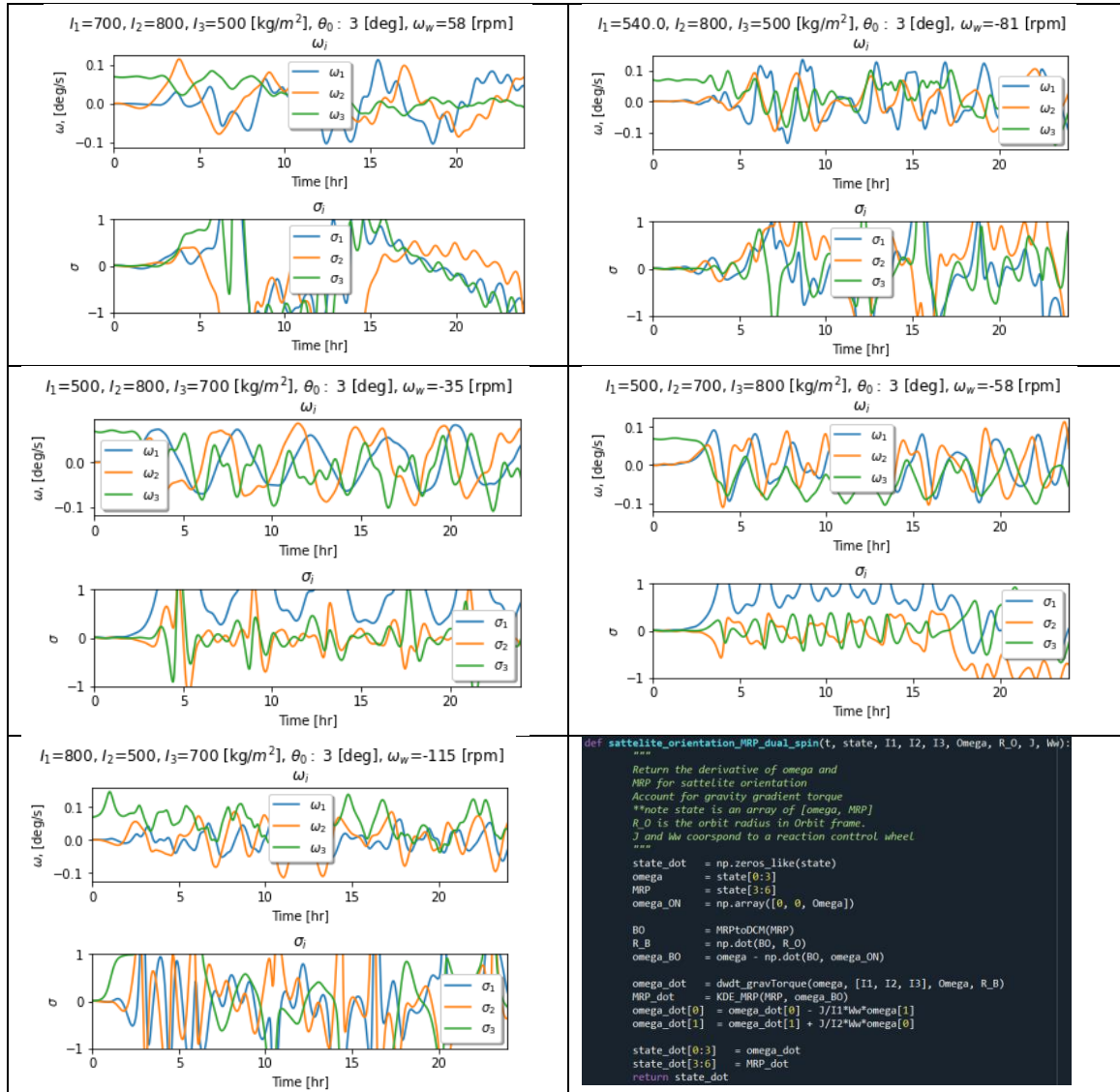
Part (h.2):

Several steps must be taken to numerically integrate the system. First, I calculate the radius vector in the B frame ${}^B\mathbf{R}$. Next, I calculate $\boldsymbol{\omega}'$. Finally, we can construct a state variable and integrate the orientation and angular velocity using the equations derived in Part (a).

$${}^B\mathbf{R} = [\mathcal{BO}(\boldsymbol{\sigma})]^O \mathbf{R} = [\mathcal{BO}(\boldsymbol{\sigma})] \begin{bmatrix} -R & 0 & 0 \end{bmatrix}^T$$

$${}^B\boldsymbol{\omega}' = {}^B\boldsymbol{\omega}_{B/O} - [\mathcal{BO}(\boldsymbol{\sigma})]^O \boldsymbol{\omega}_{O/N} = {}^B\boldsymbol{\omega}_{B/O} - [\mathcal{BO}(\boldsymbol{\sigma})] \begin{bmatrix} 0 & 0 & \Omega \end{bmatrix}^T$$

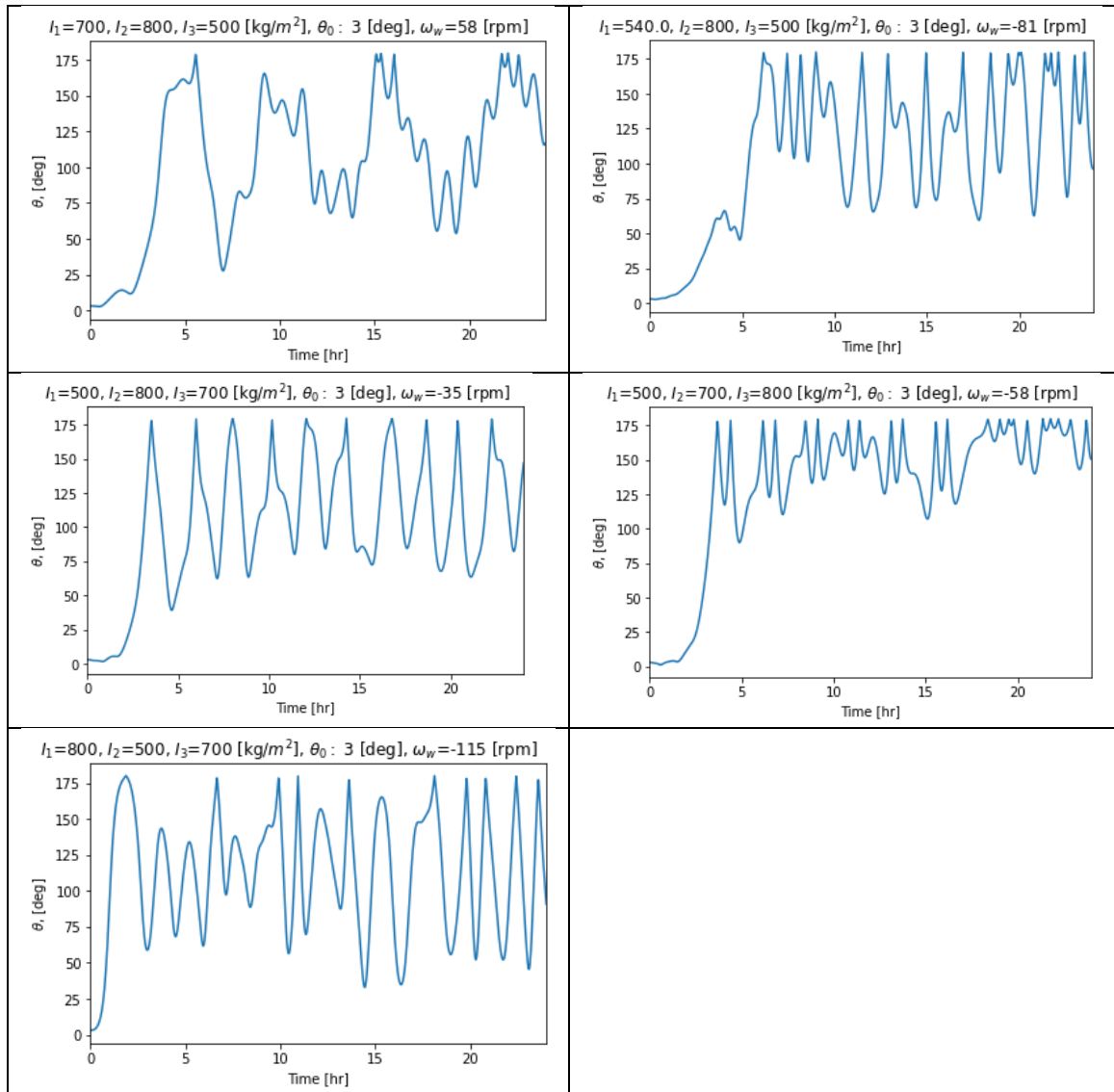
$$\begin{bmatrix} {}^B\dot{\boldsymbol{\omega}}_{B/O} \\ \dot{\boldsymbol{\sigma}} \end{bmatrix} = \begin{bmatrix} f(\boldsymbol{\omega}_{B/O}, \bar{\mathbf{I}}, {}^B\mathbf{R}) + g(\boldsymbol{\omega}_{B/O}, \bar{\mathbf{I}}, J, \omega_w) \\ h(\boldsymbol{\sigma}, \boldsymbol{\omega}_{B/O}) \end{bmatrix} = \begin{bmatrix} \text{dwdt_gravTorque() + spinTorque()} \\ \text{KDE_MRP()} \end{bmatrix}$$



Part (h.3):

Here in order to compute the angle associated with the principle axis of rotation I calculate the DCM, then the PRP from the DCM.

$$[\hat{\lambda}, \theta] = \text{DCMtoPRP}(\text{MRPtoDCM}(\sigma))$$



Part (h.4):

For all 5 scenarios we find that:

- ω, σ, θ vary significantly and appear chaotic with no discernable patterns.
- The maximum value of θ is 180 degrees which is the maximum value possible using a principle axis of rotation and selecting the shorter rotation.
- From the numerical simulation, we can say that this system agrees with our linear stability analysis which predicted that the system would be unstable for these ω_w values.
- Additionally, for the 5th case I selected a ω_w with more positive eigenvalues and we see that the results lost the coherence that was demonstrated in Part (g)

Problem 02: Problem Statement

Now, let us conduct a little deeper analysis on the attitude motion of the dual-spin satellite under gravity gradient torque. Recall that there is an important assumption in our stability analysis: the motion should follow closely the linearized differential equations for small derivations from the particular solution. We can expect that the linearized dynamics will not accurately capture the original nonlinear behaviors at some point when the deviation from the relative equilibrium state becomes “too large.”

However, it is not easy to analytically quantify how much deviation is “too large.” In addition, we can expect that the level of “too large” will be different for different values of ω_w , i.e., different ω_w would provide different levels of stability against the deviations. The aim of this problem is to numerically obtain an estimate of the “too large” level at which point the linear approximation breaks down. Throughout this problem, we assume the same orbit as in Problem 1.

- (a): Let us first design our satellite inertia properties: $\{I_1, I_2, I_3, J\}$. **Choose** and **report** a set of inertia properties $\{I_1, I_2, I_3, J\}$ (which has to be different from what we used in Problem 1) that allow at least some ω_w to yield marginal stability. **Show** the stability charts as function of ω_w/Ω to confirm that the designed satellite can be indeed stabilized by some ω_w .
Note: be careful about the possible values I_1, I_2, I_3 may take; as we learned in class, the magnitudes of K_1, K_2, K_3 must be always less than 1.
- (b): To investigate the valid regions of the linear approximation, we perform numerical simulations of the attitude motion for various ω_w and θ_0 . Recall that the initial conditions are determined by Eq. (3) for a given θ_0 . Following the guidelines stated below, **define** and **report** your test points of ω_w and θ_0 , and **mark** the instances of ω_w to be tested on the stability charts created in the previous question.
- Guidelines for the choice of ω_w and θ_0 :
 - choose at least 15 instances for each of the parameters (i.e., at least $15 \times 15 = 225$ simulations to be performed); for example, $\omega_w = \{-100, -90, -80, \dots, 90, 100\}$ rpm (21 instances) and $\theta_0 = \{1, 3, 5, \dots, 27, 29\}$ deg (15 instances).
 - Additional guidelines for the choice of ω_w :
 - choose the range of ω_w such that satisfy $\min\{\omega_w\} < -3I_1\Omega/J$ and $\max\{\omega_w\} > 3I_1\Omega/J$.
 - include ω_w that are slightly greater or smaller than the critical values of ω_w that yield $b = 0, c = 0$, or $b^2 - 4c = 0$.
- (c): For each of the test points $\{\omega_w, \theta_0\}$ defined in the previous question, numerically **integrate** the differential equations for a time span from $t = 0$ to $t = 24$ [hours] with integration tolerance 1.0×10^{-10} , **compute** the principal rotation angle $\theta(t)$, and **save** the maximum $\theta(t)$ over time, i.e., $\max_t[\theta(t)]$. **Show** a contour plot of $\max_t[\theta(t)]$ as a function of ω_w and θ_0 , with ω_w in [rpm] being the vertical axis and θ_0 in [deg] being the horizontal axis (like the one shown in Fig. 3).

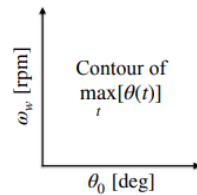


Figure 3: Contour plot of $\max_t[\theta(t)]$ as a function of ω_w and θ_0

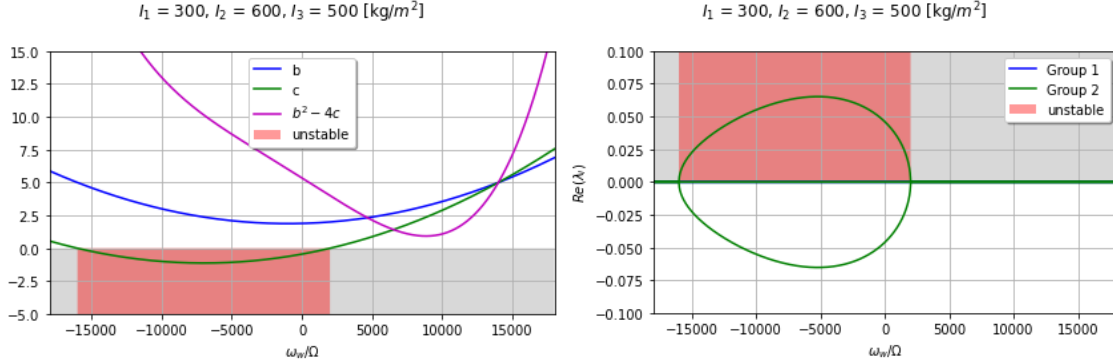
- (d): **Discuss** the obtained result, addressing the following points:
- what does the value of $\max_t[\theta(t)]$ in comparison to θ_0 tell in terms of stability?
 - what kind of trends can you find about the values of $\max_t[\theta(t)]$ as θ_0 increase (if any)?
 - what kind of trends can you find about the values of $\max_t[\theta(t)]$ as ω_w increase (if any)?
 - at what value of θ_0 do you think the result of the linear stability analysis becomes unreliable? How does that change for different ω_w ?
 - how the result would affect your design of a dual-spin satellite if the relative equilibrium state is the desired attitude of your mission?
- (e): **Choose** a few interesting results from the simulations conducted in part (c) with a fixed value of ω_w and different θ_0 , and **show** the plots of the dependent variables and $\theta(t)$ as functions of time. **Discuss** how those plots compare against each other as θ_0 increases.
- (f): In this problem, we have only considered the error in the initial attitude. In reality, there are more variety of errors that might affect the attitude motion. **Discuss** what type of errors can be considered, and what kind of influence those errors might have on the resulting attitude motion.
- (g): **Optional** (extra credit for both AAE 440 and 590)
Over the semester, we have learned various orientation representations, including direction cosine matrix, Euler angle sequence, principal rotation parameters, Euler parameters, classical Rodrigues parameters, and modified Rodrigues parameters. **Discuss** which orientation representations are your most and least favorite ones, including the reason.

Problem 02: Problem Solution

Part (a):

For this problem I will select a set of principle moments of Inertia that correspond to Region 7, which is unstable without a reaction wheel.

$$I_1 = 300, \quad I_2 = 600, \quad I_3 = 500, \quad K_1 = K_2 = 1/3, \quad K_3 = -0.6$$



Part (b):

For our case study I select 30 values for ω_w (as defined by ω_w/Ω) and 29 values for θ_0 . Then I will run the simulation for all 870 permutations defined as the cartesian product of the two sets.

Note that this $\min\left(\frac{\omega_w}{\Omega}\right) < -3I_1/J$, $\max\left(\frac{\omega_w}{\Omega}\right) > 3I_1/J$ and ω_w values that are near the $b^2 - 4c = 0$ points are included (the individual b and c inequalities are never violated for this system).

$$\frac{\omega_w}{\Omega} = \{-18,000, -16,758, \dots, 16,758, 18,000\}$$

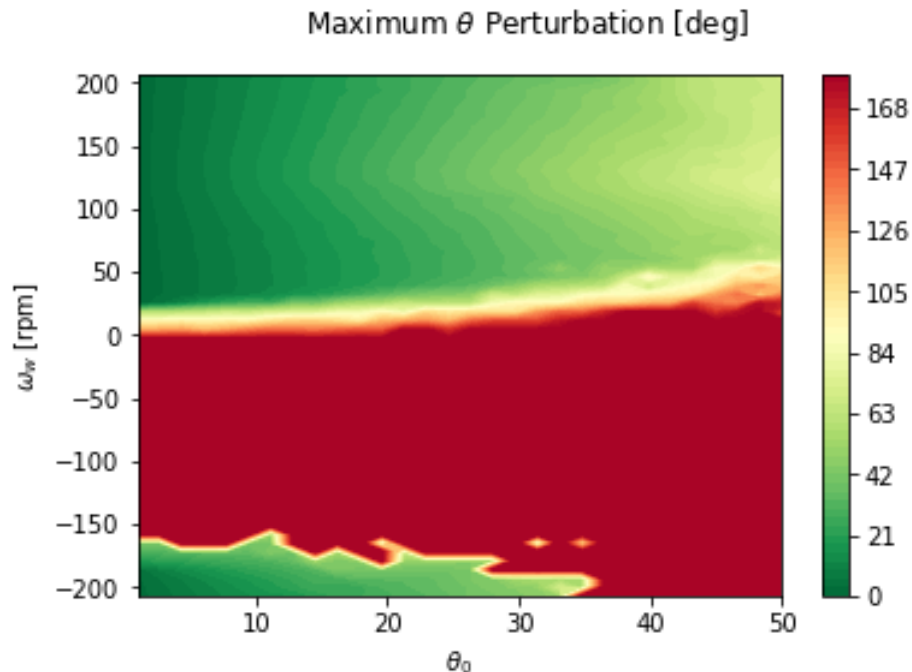
$$\omega_w \in \{-207, -193, \dots, 193, 207\} \text{ rpm}$$

$$\theta_0 = \{1, 2, \dots, 48, 49\}$$

$$\frac{\omega_w}{\Omega} \times \theta_0 = \left\{ \left(\frac{\omega_w}{\Omega}, \theta_0 \right) : \frac{\omega_w}{\Omega} \in \frac{\omega_w}{\Omega} \text{ and } \theta_0 \in \theta_0 \right\}$$

Part (c):

Next, we can simulate 24 hours of the spacecrafts attitude $\forall \left(\frac{\omega_w}{\Omega}, \theta_0 \right) \in \frac{\omega_w}{\Omega} \times \theta_0$. Then, using the attitude history we can compute the angle about the principal moment of inertia and find the maximum perturbation. Finally, we make a contour plot of initial angle, reaction wheel speed and maximum perturbation.

Part (d):

Looking at the contour plot above there are several interesting characteristics we can identify.

- Over the course of 24 hours, we find that the relative size of $\max(\theta(t))$ compared to θ_0 tells us if the system is stable. For unstable systems, regardless of the initial perturbation size, $\max(\theta(t))$ will approach 180 degrees. For stable systems, $\max(\theta(t))$ will remain close to θ_0 .
- For unstable systems $\max(\theta(t))$ hits 180 degrees, which is the maximum possible angle using PRP assuming you take the smaller rotation. For stable systems $\max(\theta(t))$ remains in the vicinity of θ_0 .
- For a given θ_0 we see that there is a region of ω_w where the system is unstable. However, increasing/decreasing ω_w beyond that belt massively reduces the perturbation and tends to reduce $\max(\theta(t))$ indicating a more stable system.
- Looking at the contour plot, we find that up until 25 degrees our linear stability analysis accurately predicts which ω_w are required for stability, but for $\theta_0 > 25$ deg, the system becomes unstable a some of these ω_w . As θ_0 increases beyond 25, the required ω_w increases.
- When designing a satellite mission, I would identify the maximum perturbation in orientation I might expect. Using this perturbation, I could find what ω_w spin rate is required to maintain stability under that perturbation. This is the rate the reaction wheel could be spun at. If this rate is too high (thousands of rpm), I may need to consider a larger reaction wheel or one capable of spinning faster to maintain satellite stability.

Part (e):

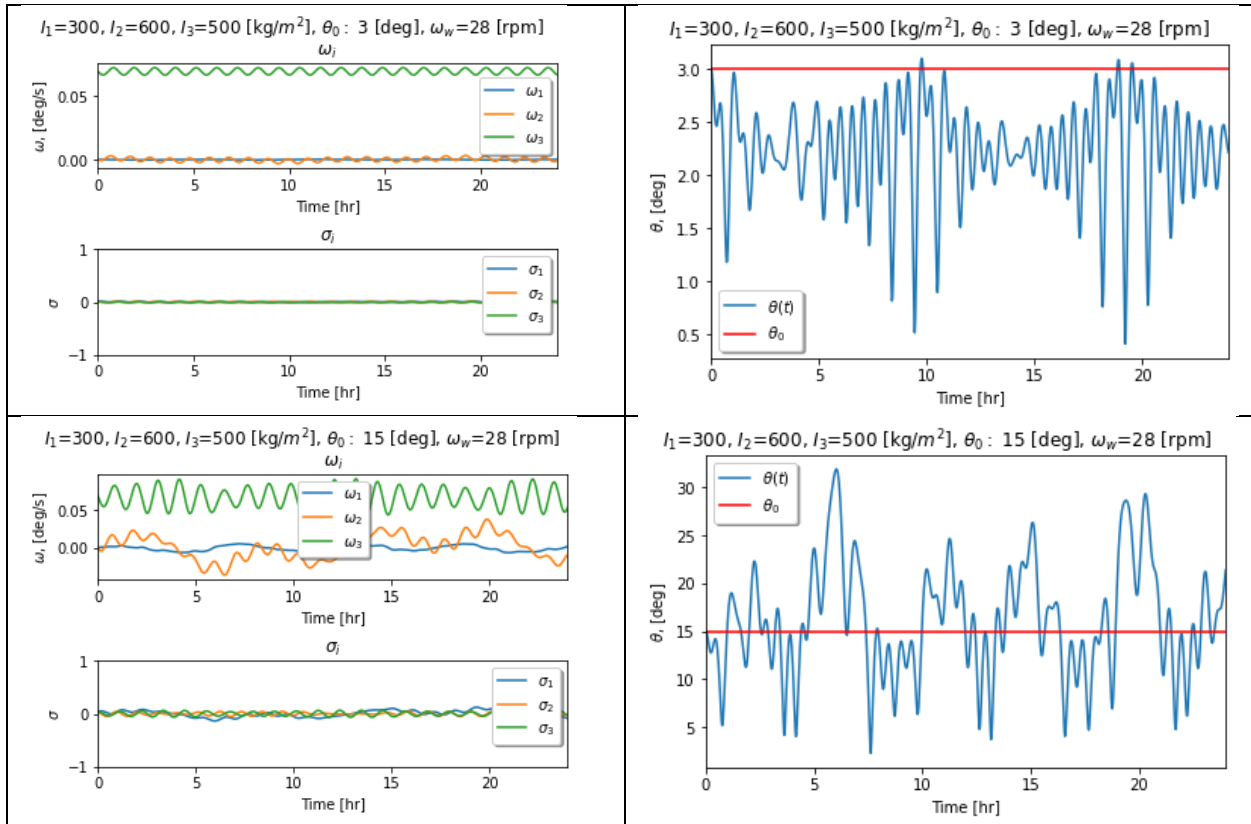
Here I wanted to look at an ω_w value that is on the border of stability and instability based on our linear stability analysis. Using our contour plot from Part (c) I selected:

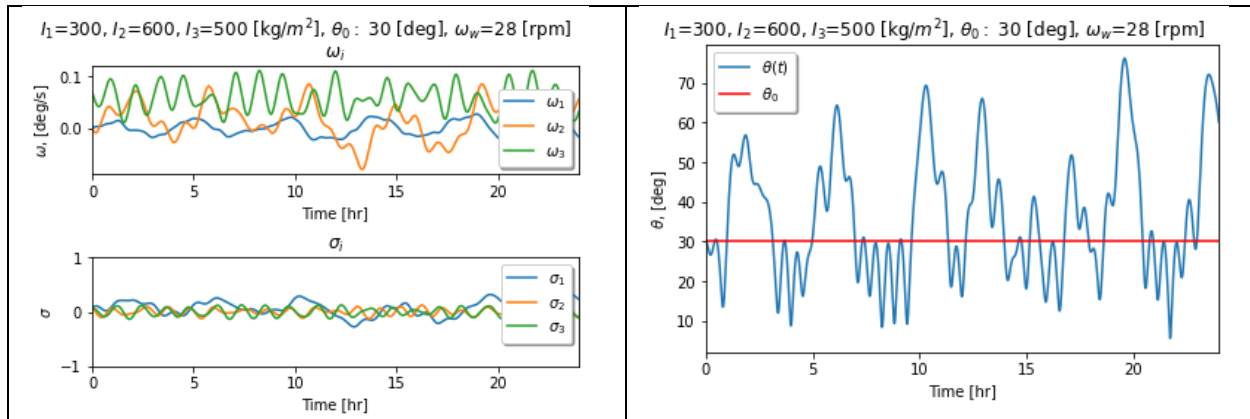
$$\omega_w = 28 \text{ rpm}, \quad \theta_0 \in \{3, 15, 30\} \text{ deg}$$

In the plots below see can see the effects of increasing our initial angle. For the small 3 degree angle the system appears highly stable. Rotation remains with ω_3 and $\theta(t)$ is bounded by θ_0 . This agrees with our linear stability analysis

For the medium 15-degree angle we see that the system begins to demonstrate some instability. Much of the angular velocity transfers from ω_3 to ω_2 and $\max(\theta)$ is more than double θ_0 .

Finally for the large angle of 30 degrees we see that the system appears unstable. This contrasts with our linear stability analysis. Here the satellites orientation varies wildly, ω_1, ω_2 and ω_3 all grow large and appear chaotic, and $\max(\theta)$ is over 90 degrees.



Part (f):

There are many other potential perturbations. One might be a perturbation in angular velocity. This could be caused by a non-perfect RCS thruster firing, micrometeorite impacts or the satellite's release from the launch vehicle. These initial perturbations could add significant rotational velocity to ω_1 and ω_2 . Another error which was not accounted for was solar pressure. This solar pressure would cause an additional torque about the center of mass changing the dynamics for $\dot{\omega}$.

Part (g):

Of all the orientation representation systems we have used in class, I find that Euler Parameters have been my favorite. I enjoy that they don't suffer from any singularity meaning the code developed for them can be applied to any system without fear of running into a singularity or having to 'switch' like with MRP. Additionally, EP's equations such as it's KDE and tend to be comparatively simple. I also enjoy Rotation Matrices and DCM as easy and critically important way for expressing vectors and matrices in a different reference frame. Lastly, I appreciate PRP because it is a very intuitive way to understand and visualize the orientation of a satellite. Generally, I liked MRP and CRP the least because of their singularities, complicated KDE, and lack of intuitive meaning.

Problem 03: Problem Statement

Students in AAE 590 should solve this problem for full score; students in AAE 440 who complete this problem with correct answers will receive extra credit.

Let us further our understanding about the attitude motion of dual-spin satellites under gravity gradient torque. Answer the following questions using some equations when necessary.

- (a): In class (also in Problem 1 and 2), we performed the linear stability analysis based on the assumption that the wheel's spin axis is aligned with \hat{b}_3 , and hence with \hat{o}_3 . **Discuss** the possibility of having the wheel rotation axis aligned with other axes, addressing the following points:
- is such a configuration useful for specific mission scenarios?
 - how would it affect the subsequent analysis (finding particular solution, performing linear stability analysis)?
- (b): Another critical assumption in our analysis is the circular orbit assumption; in general, we may also want to consider elliptic orbits depending on our mission scenarios. **Discuss** how the equations of motion and the subsequent analysis would be affected if we consider elliptic orbits.
- (c): Recall that the particular solution we have considered for our stability analysis is the relative equilibrium state, where the satellite attitude is static relative to \mathcal{O} -frame (non-inertial, rotating frame). **Discuss** what type of mission scenarios this attitude would be suited for.
- (d): Another desirable attitude includes an inertially-fixed attitude (i.e., static relative to \mathcal{N} -frame). **Discuss** what type of mission scenarios this attitude would be suited for. Also, **discuss** what you would need to do to achieve such attitude with stability.

Part (a)

Aligning the reaction wheel with another axis might be useful if the spacecraft's body axis needs to be oriented other than fixed in the \mathcal{O} frame such as for pointing towards other communication satellites the sun or deep space. If this change was made the $\dot{\omega}$ dynamic equations in Part (a) would have to be expanded where $\beta_1 \neq 0, \beta_2 \neq 0$.

Part (b)

Two key differences in an elliptical orbit are varying angular velocity and radius. These would have significant impacts on the gravity gradient torque term which relies both on Ω and R . These two terms would no longer be constant which affects the dynamic equations for $\dot{\omega}$.

Part (c)

One of the main benefits of relative stability is the satellites orientation fixed in the \mathcal{O} frame. This would allow a satellite to remain pointed towards earth throughout its orbit. This is very useful for any Earth oriented missions such as Earth photography or Earth communications.

Part (d)

One use for a satellite whose orientation is fixed in the \mathcal{N} frame is any deep space observation. This orientation would allow a camera to remain pointed at an area of the sky throughout an entire orbit.